A SIMPLE NUMERICAL METHOD TO COMPUTE THE SIGNAL-TO-NOISE RATIO OF A MAGNETIC RESONANCE IMAGING SURFACE COIL

R. Rojas and A. O. Rodriguez

Centro Nacional de Investigacion en Instrumentacion e Imagenologia Medica
Universidad Autonoma Metropolitana Iztapalapa
Ave. San Rafael Atlixco 186, Mexico, DF 09340, Mexico

Abstract—The quality of a magnetic resonance image can be reliably measured by the signal-to-noise ratio. This widely accepted parameter is a function of the magnetic field generated by the coil and the electric field produced by the sample to be imaged. A simple numerical method is proposed to calculate the coil signal-to-noise ratio of a circular-shaped coil and a spherical phantom. The phantom is composed of two-concentric sphere simulating a brain-skull model. The electromagnetic fields produced were then numerically computed by solving Maxwell's equations with the finite element method implemented in a commercial software tool. The electric and magnetic fields were used to numerically determine the signal-to-noise ratio using the quasi-static approach. The numerical results demonstrated that this simple method is able to calculate the signal-to-noise ratio of surface coils with simple coil geometries involving a simulated phantom.

1. INTRODUCTION

The Radio Frequency (RF) resonator coils are a fundamental device of a Magnetic Resonance Imaging (MRI) system. The quality of the MR images strongly depends on the signal-to-noise ratio (SNR) of the acquired signals normally obtained with a receiver coil [1]. The SNR is the widely accepted parameter for measuring coil performance. This parameter involves both the MRI signal and the associated noise generated by different sources [2].

Corresponding author: A. O. Rodriguez (arog@xanum.uam.mx).

Analytical expressions can be derived from the classical electromagnetic theory for the simplest cases of surface coils [3]. The classical electromagnetic theory poses mathematical challenges usually extremely difficult to solve for more complex geometries. The complexity of the problem increases when the coil is nearer the sample and the electromagnetic properties of the environment modifies the distribution of *SNR*. An analytical solution even for the unloaded coil case is extremely difficult to derive. Alternatively, numerical solutions have been proposed in the past with good results [4].

The simulation of the electromagnetic properties of MRI coils represents a good alternative to both the derivation of analytical expressions and, the trial-and-error scheme to study the coil performance. A number of numerical approaches have been developed to solve various electromagnetic problems and applications [5].

Numerical solutions to Maxwell's equations can be classified into two main approaches: 1) the integral equation model, and 2) the differential equation model [6]. The are a number relevant numerical methods: a) The Finite Integration Technique (FIT) requires the discretisation of the integral forms of Maxwell's equations to transform them into a set of matrix equations. The current equations contain topological information, and the constitutive equations are expressed in terms of matrices that depend on dielectric and magnetic properties of the media and, relate the voltages of the fluxes. b) In the Finite Difference (FD), Maxwell's equations are solved by dividing the region of interest into uniformly-sectioned small rectangular grids and then employing a set of linear equations together with an iterative method. c) The Finite Difference Time Domain (FDTD) is an extension of the method described in b) and is applied in the time domain. This involves spatially sampling the electric and magnetic field distributions over the volume of interest by enclosing it in a rectangular box. The box is divided into many small rectangular cells and the calculation is performed over a given time period. This method is easy to implement but loses accuracy for arbitrary geometries. d) The Method of Moments (MoM) is a frequency domain method and in computational electromagnetics it has become synonymous with the integral-differential operator equations. It operates in terms of a volumetric equivalent current that accounts for the effect of the permittivity and conductivity of an inhomogeneous body. This method is popular for arbitrarily-shaped and inhomogeneous dielectric bodies. e) The Finite Element Method (FEM) is a differential equation approach in which the complete problem, source geometry, excitation, scatterers and boundary constraints, is discretised in a variable manner. FEM divides the region of interest into irregular

triangular cells. It does not loose accuracy for abritray geometries. Then FEM can accurately model arbitrary geometries with small mesh elements used to describe complex geometries and larger mesh elements used in more uniform regions. The trial function is a combination of a set of base functions defined over subdomains (the mesh elements) that comprise the entire problem domain. Thus, the field equations are determined in terms of polynomials with unknown coefficients defined in the mesh nodes or along element edges. These unknown coefficients are then determined solving a matrix equation system. Since the shape of the triangular cells can be arbitrary in FEM, we have used it to numerically simulate the electromagnetic behavior of different geometries (polygonal shapes) of a single loop RF surface and arrays coil designs [7, 8]. FEM is suitable to solve complex problems frequently found in electromagnetic theory.

In this paper, we proposed a simple numerical method to compute the SNR generated by a single loop coil interacting with a pixel-based model of two concentric spheres emulating a brain-skull model. The SNR is computed via the calculation of the electric and magnetic fields of the coil-sphere system in a three-dimensional Cartesian space. We used a commercial software tool based on the FEM to solve Maxwell's equations.

2. METHODS

2.1. The Mathematical Model

A mathematical model to numerically compute both the electric and magnetic fields was derived using Maxwell's equations. It is important to highlight that the model presented here was then transformed into descretised form to be solved with the FEM and it is solely for the quasi-static approach. The crucial criterion for the quasi-static approximation to be valid, is that the electromagnetic fields are practically the same at every instant as if they had been generated by stationary sources. This implies that the currents and charges generating the electromagnetic fields vary slowly in time.

Under these assumptions, Maxwell's equations can be simplified and their numerical solution can be obtained from:

$$\sum_{i=1}^{N} A_{zi} \int \int_{\Omega} \left[\bigtriangledown N_i \cdot \bigtriangledown N_j + \omega\mu(\omega\varepsilon - j\sigma)N_i N_j \right] dxdy$$

$$= -\int \int_{\Omega} \mu N_i J_z^e dxdy \tag{1}$$

where Ω is the integration region, J^e is a current density generated externally, σ is the medium conductivity (S/m), μ is the medium permeability (H/m), ε is the medium permittivity (F/m), ω is the Larmor frequency and, ρ is the electric charge density (C/m^3). A_{zi} is the vector potential along the z-direction for the nodal number, i. N_i and N_j are the expansion nonzero functions associated with the node, i. A complete derviation of Equation (1) is in Appendix A. The term on the right-hand side of Equation (1) can be defined as G_{ij} and the left-hand side as b_i. Finally, Equation (1) becomes

$$\sum_{j=1}^{N} G_{ij} A_{zi} = b_i \qquad (2)$$

Equation (2) represents only the solution along the z-direction, however similar expressions can be found for the x and y axes. A set of linear equations can be formed for this direction and solved using a matrix system. To numerically compute the magnetic and electric fields, the vector potential A_{zi} and Equations (A9) and (A10) together with a software tool were used.

2.2. Electromagnetic Simulation

The graphic interface of the commercial software tool COMSOL multiphysics [9] was used, to build a spherical phantom to mimic the brain and skull and the circular coil. The three-dimensional structure was developed using regular geometrical figures such cylinders, cubes, etc. The skull and the brain were represented in the model of Fig. 1 by concentric spheres of 13 cm radius and 12 cm of radius, respectively. The MRI surface coil had the following dimensions: thickness of 0.1 cm, inner radius of 6.0 cm and external radius 9.0 cm. The origin of co-ordinates system was located at the inner sphere centre. Fig. 1 shows the pixel brain-skull model and the surface coil model used to numerically compute both the electric and magnetic fields. The conductive spheres representing the head produce changes in the impedance as a function of the sample electrical properties: σ and ε. RF coils are normally made out of copper, so $\sigma = 5.998 \times 10^7$ S/m and $\varepsilon_r = 1$ were used. The three-dimensional model was surrounded with an outer sphere of 20 cm of radius representing boundaries for the simulation process, where the gap between the sphere arrangenment and the boundary was assumed to be filled with air. Different electric and magnetic properties for each element in the model were used as the frequency was modified in the simulations. Electrical conductivity and permittivity values for brain and skull were taken from [10]. Current
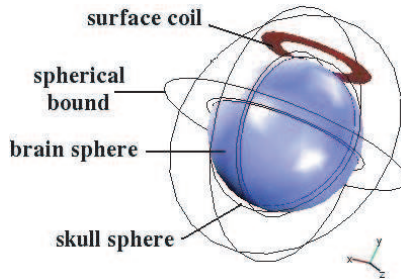
Figure 1. Three-dimensional skull-brain model. The inner sphere represents the brain cavity, the outer sphere represents the skull-head, and the circular ring represents the copper coil. The external sphere represents the system envelope (spherical bound).

densities at different radio frequencies were applied at one time, then the software tool calculated the electric and magnetic fields of the sphere-and-coil model. To numerically solve our problem, tetrahedrals were used to form the mesh to fully cover the entire three-dimensional model.

2.3. Mesh Construction

The FEM divides the three dimensional domains into a mesh of small tetrahedric subregions or finite elements. Usually, four nodal points are associated with each element at the corners of the tetrahedral. An advantage of using tetrahedral elements is that they can be made to fit any shape of domain boundary to a very good accuracy, which can easily be increased y increasing the number of elements (Fig. 2(a)). The element size and shape are defined by the geometry under study, each element and its nodes are numbered with different sequences [11]. Fig. 2(b)) shows the final mesh configuration used in this work. The solution of three-dimensional electromagnetic problems requires great computing power. Extra care should be taken when selecting the type of mesh. An arbitrary mesh is not recommended since for the coarsest mesh the iterative process may not easily converge. A minimum requirement is that there should be at least two mesh elements per wavelength in the geometry according to the Nyquist criterion. The highest frequency in this work was 100 MHz with a wavelength of 3 m. The radiation-matter interaction depends on the material properties and the wavelength, and the mesh has to resolve the wave across the whole geometry.
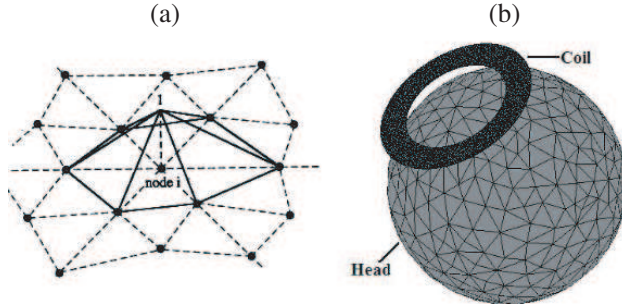
(a)   (b)

Figure 2. In FEM modeling the computational domain is discretised into tetrahedral elements where each tetrahedral corresponds to an element (a). The mesh construction with the tetrahedral meshing for the three-dimensional pixel model is in (b).

2.4. Signal-to-noise Ratio Calculation

A set of nuclear spins precessing inside the sample, induce an EMF at the coil proportional to the resonant frequency, ω that depends on principal magnetic field B_0. The number of spins is proportional to the sample volume V, and the coupling between nuclei and the coil depends on the magnetic field of the RF, B_1. The noise is proportional to the effective resistance R_{efec} including the interaction with the body. Hoult and Richards proposed [1]:

$$SNR = \frac{V\omega^2 B_1}{R_{efec}} \qquad (3)$$

The noise level is determined by dissipative power losses in the system, such as conductor, radiation, and overall body losses. The fluctuation dissipation theorem states that there exists a direct relationship between electrical resistance and noise. The thermally activated motions of the charge carries in dissipative media produce random electric and magnetic fields which can be detected as noise.

A resistance R produces an RMS noise voltage V_n given by $V_n = \sqrt{4\kappa T \Delta f R}$, where κ is Boltzmann's constant, T is absolute temperature, Δf is the receiver bandwidth, and $R = R_A + R_B$, where R_A and R_B are the real part of the input impedance of the RF coil itself and the sample respectively [7]. From Equation (3) and the definiton of the RMS voltage, the SNR can be rewritten as:

$$SNR = \frac{V\omega^2 B_1}{\sqrt{4\kappa T \Delta f (P_A + P_B)}} \qquad (4)$$

where the power losses are P_A (coil) and P_B (biological sample). The energy dissipation per volume unit is approximately $P_A = I^2 R_A$ and $P_B = I^2 R_B$ [4], then:

$$\frac{dP}{dV} = \sigma E^2 \tag{5}$$

Then, a good aproximation to compute the *SNR* at a particular cpoooinrdt can be obtained combining Equations (4) and (5):

$$SNR \propto \frac{B_1\,(\text{magnetic field})}{E\,(\text{electric field})} \tag{6}$$

Equation (6) implies that it is necessary to compute the magnetic field $B_1(r)$ and the electric field E. Once both fields were computed as described in Section 2.2, bi-dimensional mapping data were represented by matrices: $[B_1(i,j)]$ and $[E(i,j))]$ where (i,j) corresponds to the Cartesian coordinates of the magnetic and electric fields at a particular position. Then, the *SNR* can be written

$$SNR(i,j) \propto \frac{B_1(i,j)}{E(i,j)} \tag{7}$$

Equation (7) implies that the *SNR* is computed by diving every matrix entry in an arithmetical fashion rather than using a matrix operation. These matrices were finally used with specially written programmes in MATLAB (V. 6.5, MathWorks, Inc) to determine the *SNR*. All simulations were performed on a Windows-operated PC. An alternating current of 1 A was applied to the circular coil for simplicity at the frequency of 100 MHz.

3. RESULTS AND DISCUSSION

It was possible to derive a discretised expression as a function of the vector potential along the z-direction from classical electromagnetic theory, which was reported by the commercial package COMSOL we found no evidence of similar work having been published previously. Discretised expressions for the x- and y-directions can also be derived. Equations in each direction were numerically solved using COMSOL, which employs the finite element method together with tetrahedrical elements to simulate electromagnetic fields in a three-dimensional space. The tetrahedral elements can take different sizes to fit a particular arrangement to be studied with a certain degree of accuracy. The accuracy depends on the number of tetrahedrals used in a particular mesh.

The mesh in Fig. 2(b) was used to cover the head-coil setup with a reasonable number of tetrahedral elements for the numerical computation of both fields as summarized in Table 1. A single tetrahedral elements had a volume of $2.5\,\mathrm{cm}^3$. The size of the elements is in good concordance with the Nyquist criterion as mentioned in Section 2.3. Since only regular figures were used the dimensions of the mesh elements across the setup did not vary drastically. Most mesh generation schemes use a mesh refinement technique to represent fine structures with much smaller elements. The mesh refinement allows us to obtain a more accurate solution. However, this tends to increase the number of nodes and elements, thus demanding overwhelming computation capabilities. One regular refinement can be sufficient to obtain a good approximation. All numerical simulations were done using a coarser mesh with the same size as summarized in Table 1.

Table 1. Number of elements used for all simulations.

Structure	No. mesh elements
Brain sphere	1240
Skin sphere	1217
Surface coil	3875
Boundary sphere	1244
Total number	23 267

As a demonstration of the presented methodology, the magnetic and electric fields were numerically computed using the three-dimensional model of Fig. 1 and mesh configuration of Fig. 2(b). Bidimensional plots in the x-y plane of both fields generated by the RF coil and the sample at 100 MHz are shown in Figs. 3(a) and (b). The numerically-simulated fields in the coronal orientation show that the field uniformity decreases at the centre of the model for both electric and magnetic fields. The intensity of the electric and magnetic fields is higher near the coil boundaries, and decreases towards the coil centre. On the other hand, a good coil design should produce a very low electric field and a high magnetic field to be able to generate a good quality image. This is an expected pattern typically found in the design of surface RF coils normally used for various MRI applications. Additionally, our approach is able to show section through at almost any location and in any arbitrary plane as shown in the top row of Fig. 3(a).

With the field mapping data of Fig. 3 and Equation (7), *SNR* maps were finally computed for a resonant frequency of 100 MHz. The
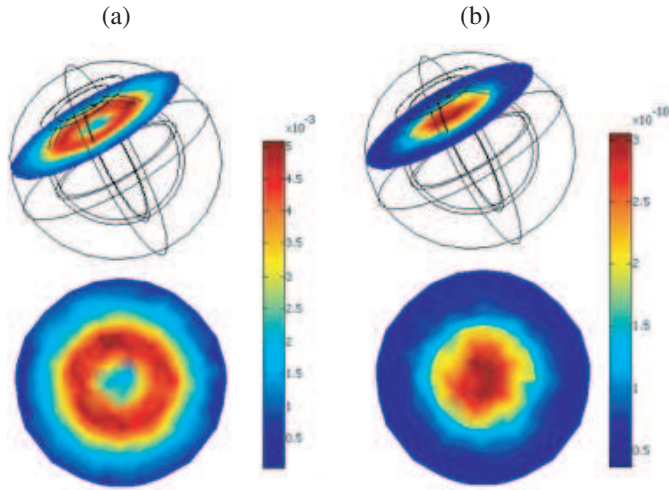
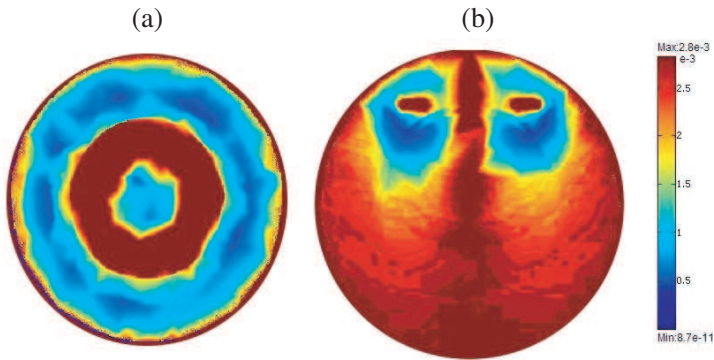**Figure 3.** The electric and magnetic fields simulated at 100 MHz and 8 cm away from the coil plane.

Figure 4. Bi-dimensional mappings of the numerically-acquired *SNR* are shown in axial (a) and coronal (b) orientations for the resonant frequency of 100 MHz.

numerically-computed *SNR* is shown in the form of bi-dimensional maps in Figs. 4(a) and (b) for the 100 MHz case. These numerical results compare very well with those reported in the literature using other numerical approaches [4]. A major drawback is the size of the mesh, and necessarily the number of elements implied in the simulation. The selection of the right mesh size may determine

the feasibility of this method, since the finer the mesh the more computational power required. The FEM becomes even more demanding as the resonant frequency is increased limiting the study of surface coil performance at magnetic fields lower than 100 MHz with a standard PC.

The spherical brain-skin model is one of the most simple models. However, this procedure can be applied to more realistic human-head models. It still remains to be investigated if by refining the mesh a significant accuracy can be obtained with our method. Consequently, the use of a computer cluster is mandatory as has been shown by other research groups.

Despite all those technical limitations imposed by the FEM and, the limited computational capacity it was possible to numerically compute the SNR of a setup involving the biological sample. This is an important advantage since the actual biological sample can be included, offering more realistic results to study the coil performance without a great deal of computer resources. This approach offers a simple and easy-to-follow methodology to calculate the SNR of an MRI surface coil. A good alternative to investigate coil performance should include pixel-based models of organs and tissues for more realistic situations and to be able to be compared with experimental results.

4. CONCLUSIONS

The numerical method presented in this work offers a simple way to compute the SNR of common geometry surface coils for MRI involving a simulated phantom too. The results show the feasibility of using a commercial software package to numerically simulate the electromagnetic properties of surface coils for MRI. This method can extended to other organs and tissues together with more complex coil configurations.

ACKNOWLEDGMENT

APPENDIX A. CALCULATION OF TIME-HARMONIC, QUASI-STATIC MAGNETIC AND ELECTRIC FIELDS

From Maxwell-Ampere's law combined with the Lorentz force equation applied to current density, J, for a quasi-static system, an equation relating the magnetic and elecrtic fields can expressed as follows:

$$\bigtriangledown \times H - \frac{\partial D}{\partial t} = \sigma(E + \nu \times B) + J^e \tag{A1}$$

where H is the magnetic field intensity (A/m), D is the electric displacement (C/m^2), J is the current density (A/m^2), σ is the medium conductivity (S/m), E is the electric field intensity (V/m), ν is the relative velocity of the reference system (m/s), B is the magnetic field density (Wb/m^2) and, J^e is a current density generated externally (A/m^2).

Expressing the magnetic and electric fields in terms of the magnetic vector potential (A) and the electric scalar potential (V)

$$B = \bigtriangledown \times A \tag{A2}$$

$$E = -\bigtriangledown V - \frac{\partial A}{\partial t} \tag{A3}$$

The complete constitutive equations for the magnetic and electric fields are:

$$B = \mu(H + M) \tag{A4}$$

$$D = \varepsilon E + P \tag{A5}$$

where, M is the magnetization vector (A/m), P is the electric vector polarization (C/m^2). But remembering that the magnetization and polarization are properties of the medium, we assumed for simplicity that the human brain produces a negligible effect. Using the constitutive Equations (A4) and (A5) in (A1) we obtain:

$$\bigtriangledown \times (\mu^{-1}B - M) - \frac{\partial(\varepsilon E + P)}{\partial t} = \sigma(E + \nu \times B) + J^e \tag{A6}$$

Using Equations (A2) and (A3) in Equation (A6), it then transformed into:

$$\bigtriangledown \times \left(\mu^{-1}\bigtriangledown \times A - M\right) - \frac{\partial\left(\varepsilon\left(-\bigtriangledown V - \frac{\partial A}{\partial t}\right) + P\right)}{\partial t}$$
$$= \sigma\left(-\bigtriangledown V - \frac{\partial A}{\partial t} + \nu \times \bigtriangledown \times A\right) + J^e \tag{A7}$$

Considering a non-magnetic ($M = 0$) and non-polarized ($P = 0$) medium, a non-moving geometry ($\nu = 0$) and no external electric gradient potential ($V = 0$, this is the ground boundary condition used for symmetry boundaries) and reordering terms of the equation, Equation (A7) becomes:

$$\sigma \frac{\partial A}{\partial t} + \varepsilon \frac{\partial^2 A}{\partial t^2} \bigtriangledown \times \left(\mu^{-1} \bigtriangledown \times A\right) = J^e \tag{A8}$$

A time-harmonic function using the Euler's formulation can be written in the form: $A(r,t) = Re\left[A(r)\exp j(\omega t + \phi)\right]$, where ϕ is the phase angle, and $A(r)\exp j\phi$ is the phasor, using this function in Equation (A15) we obtain:

$$\omega(j\sigma - \omega\varepsilon)A + \bigtriangledown \times \left(\mu^{-1} \bigtriangledown \times A\right) = J^e \tag{A9}$$

However, A is the magnetic potential so $\bigtriangledown \cdot A = 0$. Now, Equation (A9) can be rewritten along the z-direction

$$\bigtriangledown^2 A_z + \omega\mu(j\sigma - \omega\varepsilon)A_z = \mu J_z^e \tag{A10}$$

The FEM does not actually solve Equation (A10). The numerical solution corresponds to the values of known quantities at the the nodes or edges of the discretised domain. The solution is finally obtained by solving a set of linear equations using scalar functions (e.g., Equation (A10)) for each direction in the Cartesian plane and in their corresponding integro-differential formulation. These equations are solved either by minimisation or using the weighted residual method (WRM) that requires of functions $W(x,y)$ denominated weighted functions. If we applied a weighted function to Equation (A10) and using surface integral, it becomes

$$\int\int_\Omega W(x,y)\left[\bigtriangledown^2 A_z - \omega\mu(\omega\varepsilon - j\sigma)A_z\right]dxdy = \int\int_\Omega W(x,y)\mu J_z^e dxdy \tag{A11}$$

Using the vector identity $\bigtriangledown \cdot (W \bigtriangledown A_z) = W \bigtriangledown^2 A_z + \bigtriangledown W \cdot \bigtriangledown A_z$ and Gauss' theorem can help us to simplify equation (A.11) which can be rewritten as follows

$$\int\int_\Omega \left[\bigtriangledown W \cdot \bigtriangledown A_z + W\omega\mu(\omega\varepsilon - j\sigma)A_z\right]dxdy$$
$$= \oint_C W\frac{\partial A_z}{\partial z}dl - \int\int_\Omega W\mu J_z^e dxdy \tag{A12}$$

FEM assumes that the electric field vanishes at the boundary of the region of interest, so the solution only considers the interior of the

region of interest. To find the numerical solution of Equation (A12), for the electric field, a A_{zi} value is assigned for each internal node, where i denotes the nodal number (see Fig. 2). Additionally, it is assumed that the field in each element is a linear extrapolation of the three elements compromising the node. From these assumptions, the potential A_z can be written in a discrete formula

$$A_z(x,y) = \sum_{i=1}^{N} N_i(x,y) A_{zi} \tag{A13}$$

where N is the total number of internal nodes and $N_i(x,y)$ is the expansion nonzero function associated with node, i. Equation (1) can be derived using Equations (A12) and (A13).

REFERENCES

1. Hoult, D. I. and R. E. Richards, "The signal-to-noise ratio of the nuclear magnetic resonance experiment," *J. Magn. Reson.*, Vol. 24, 71–85, 1976.

2. Hoult, D. I., "Sensitivity and power deposition in a high-field imaging experiment," *J. Magn. Reson. Imaging*, Vol. 12, 46–67, 2000.

3. Ocegueda, K. and A. O. Rodriguez, "A simple method to calculate the signal-to-noise ratio of a circular shaped coil for MRI," *Con. Magn. Reson.*, Part A, Vol. 28A, 422–429, 2006.

4. Jin, J., *Electromagnetic Analysis and Design*, CRC Press, Boca Raton, 1985.

5. Li, B. K., F. Liu, E. Weber, and S. Crozier, "Hybrid numerical techniques for the modelling of radiofrequency coils in MRI," *NMR Biom.*, in press, 2009.

6. Hand, J. W., "Modelling the interaction of electromagnetic fields (10 MHz–10 GHz) with the human body: Methods and applications," *Phys. Med. Biol.*, Vol. 53, 243–286, 2008.

7. Rojas, R. and A. O. Rodriguez, "Finite-element electromagnetic simulation of a volume resonator coil for MR neuroimaging," *27th IEEE EMBS Conf.*, 1659–1662, 2005.

8. Rojas, R. and A. O. Rodriguez, "Numerical study of the optimal geometry of MRI surface coils," *29th IEEE EMBS Conf.*, 3890–3893, 2007.

9. FEMLAB Reference Manual, 2nd Edition, COMSOL Multiphysics, Burlington, MA, USA, 2005.

10. Gabriel, S., R. W. Lau, and C. Gabriel, "The dielectric properties of biological tissues: III. Parametric models for the dielectric spectrum of tissues," *Phys. Med. Biol.*, Vol. 41, 2271–93, 1996.

11. Fenner, R. T., *Finite Element Methods for Engineers*, 38, The MacMillan Press LTD, London, 1975.